Soft Matter

PAPER

View Article Online
View Journal | View Issue

The force of impacting rain†

Cite this: *Soft Matter*, 2014, **10**, 4929

Dan Soto,[ab] Aurélie Borel De Larivière,[ab] Xavier Boutillon,[c] Christophe Clanet[ab] and David Quéré[ab]

Received 6th March 2014
Accepted 9th April 2014

DOI: 10.1039/c4sm00513a

www.rsc.org/softmatter

Drop impacts are difficult to characterize due to their transient, non-stationary nature. We discuss the force generated during such impacts, a key quantity for animals, plants, roofs or soil erosion. Although a millimetric drop has a modest weight, it can generate collision forces on the order of thousand times this weight. We measure and discuss this amplification, considering natural parameters such as drop radius and density, impact speed and response time of the substrate. We finally imagine two kinds of devices allowing us to deduce the size of the raindrop from impact forces.

Drop impacts have been recently studied due to their ubiquitous implication in everyday life. For printing, coating or spraying, from pesticides to rain,[1,2] it is essential to understand the collision mechanisms of a drop. Many aspects have been and are still explored.[2,3] Special attention has been given to the early stages of the splash,[4,5] to the dynamics of the spreading radius,[6] or to the influence of the substrate.[6–10] However, the force experienced by a substrate hit by a drop has been less discussed, apart from early discussions about soil erosion[11–13] and more recent studies about the rain impact on small creatures.[14]

It is reasonable to assume that the heavier the drop, the stronger the impact force F, so that the drop radius R and density ρ naturally arise as key parameters in the study. Conversely, understanding the force F may allow us to deduce drop radii for a given liquid, providing a new kind of "disdrometer" – namely, the device giving access to the size distribution of rain. Drops in this study are formed by means of a syringe and various needles which provide radii between 1 and 2 mm. The syringe is fixed to a vertical beam and its height varies so as to generate impact speeds V from 20 cm s^{-1} to 6 m s^{-1} (close to the terminal speed of middle-size raindrops). We record the impact from the side with a fast camera, using backlighting to enhance the contrast (Fig. 1a, or ESI Movie 1†). By this means, we access the impinging speed of the drop and can check the centering of the impacts. In order to control the impact position with a precision of more than 1 mm, even for high falls, two perpendicular micrometric screws are placed between the syringe and the beam.

The main specificity of this study dwells on the impulsive character of the event. A first characteristic time is the "crashing time" $2R/V$ of the drop, typically 1 ms in our experiments. We assume here that this time is smaller than the Rayleigh time of vibration of the drop, which corresponds to typical impact velocities larger than 20 cm s^{-1}. Denoting c as the speed of sound in the drop, a third characteristic time related to compression waves and to the water hammer phenomenon[1,11,15,16] can be constructed. These waves are likely to generate huge pressures (on the order of MPa) on a duration scaling as $2RV/c^2$ (ref. 11 and 17) (several ns), that is, the time for the shockwave to reach the spreading edge of the contact area. Therefore the corresponding maximum contact area scales as $(RV/c)^2$, resulting in tiny forces of the order of the μN. In addition, recent experiments[18,19] with a micro-second resolution and theoretical studies[20] have shown that air discs can be entrapped under the center of the drop, which affects the singularity at the contact and thus the pressure and impact force at very short time.

We measure the impact force with a piezoelectric quartz: an impact hammer, PCB Piezotronics Model 086D80, is diverted from its normal usage and the signal is delivered *via* a Kistler charge amplifier 5015A such as used in ref. 11,12 and 21 with a cut-off frequency of 10 kHz. The signal obtained after impact is recorded by a digital oscilloscope having a time resolution of the order 50 μs. This resolution does not allow us to extract any information regarding air entrapment. We show in Fig. 1b a typical profile of the impact force as a function of time, for a water drop with $R = 1.30 \pm 0.02$ mm, $\rho = 1000$ kg m^{-3} and an impacting speed $V = 3.00 \pm 0.02$ m s^{-1}. We observe that the typical force (50 mN for millimetric water drops) is several orders of magnitude larger than the one generated by a water hammer pressure.

From now on, F_0 denotes the maximum force of impact measured on curves similar to Fig. 1b. In order to obtain a larger signal, even at modest speed or small radius, we choose a liquid

[a]*Physique et Mécanique des Milieux Hétérogènes, UMR 7636 du CNRS, ESPCI, 75005 Paris, France*
[b]*Ladhyx, UMR 7646 du CNRS, École Polytechnique, 91128 Palaiseau Cedex, France*
[c]*Laboratoire de Mécanique des Solides, UMR 7649 du CNRS, 91128 Palaiseau Cedex, France*

† Electronic supplementary information (ESI) available. See DOI: 10.1039/c4sm00513a

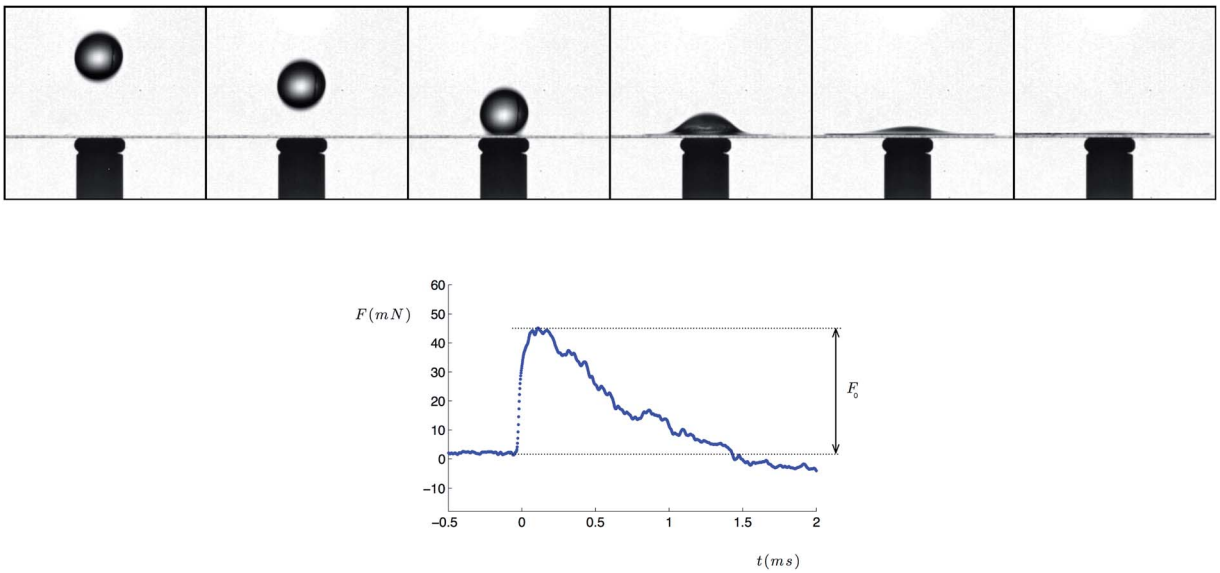

Fig. 1 (a) Side view of a water drop of radius $R = 1.3$ mm hitting a piezoelectric quartz at $V = 3$ m s^{-1}. Images are separated by 0.5 ms from which we extract the impact velocity V. (b) Impact force F as a function of time for this experiment, measured by the piezoelectric sensor. The origin of time is chosen at contact. Impingement typically lasts for $2R/V \approx 1$ ms, the time needed for the drop to travel by its own diameter. The curve is not symmetrical between the beginning and the end of the collision. The maximum force F_0 is reached after about a tenth of a millisecond.

denser than water: an eutectic gallium–indium–stain alloy (Ga : In : Sn; 62 : 22 : 16 wt%) commonly called Galinstan,[22] recently used for studying impact dynamics.[23] This liquid metal at ambient temperature is six times denser than water ($\rho = 6359$ kg m^{-3}) and has a viscosity of 2 mPa s, close to that of water. Repeating the experiment of Fig. 1 for different drops and impact speeds yields Fig. 2a, where the maximum force F_0 for Galinstan is plotted as a function of V for three radii. The typical value of F_0 becomes now 300 mN, which corresponds to one thousand times the drop weight. We observe that F_0 evolves as V^2 (dotted lines in Fig. 2 are parabolic fits in log–log scale), a signature of the inertial nature of the collision. Hence the liquid density should also matter, and we compare in Fig. 2b the function $F_0(V)$ for Galinstan and water, at a fixed radius $R = 1.3$ mm. The parabolic behaviour is independent of the liquid nature, and it is found that F_0 is 6 times greater for Galinstan than for water at any impact speed, corresponding to the density ratio between these two liquids. Studies in the 80s by Nearing,[11,12] and more recently by Grinspan & Gnanamoorthy,[21] obtained comparable results with water only and on a much more narrow range of velocity, making it difficult to extract scaling laws in velocity. In 2012, numerical and experimental studies performed by Mangili *et al.*[24] suggested different predictions for the force of impact. Our measurements are in good agreement with their numerical simulations assuming potential flow theory.

According to these results, we propose a model based on an inertial scenario, as postulated in ref. 13. During impact, the

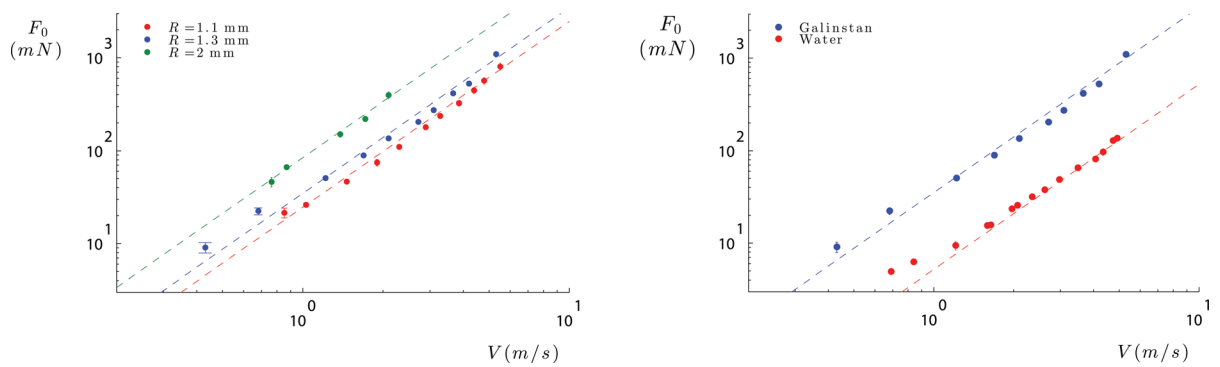

Fig. 2 (a) Maximum force F_0 at impact as a function of the collision speed V for Galinstan, an alloy of indium, gallium and stain. F_0 is typically 300 mN, that is, about 1000 times the weight of the drop. The dashed lines show eqn (1) without any adjustable parameter. (b) F_0 as a function of V for Galinstan and water at fixed drop radius ($R = 1.3$ mm). Whatever the impact speed, forces differ by a factor 6, approximately the ratio between the two liquid densities. Again, the dashed lines show eqn (1).

transmitted quantity is momentum: at a given time, a slice of drop of height $V\mathrm{d}t$, radius $r(t)$ (that changes from 0 to R) and mass $\mathrm{d}m = \rho\pi r^2(t)V\mathrm{d}t$ decelerates from V to 0 in a time $\mathrm{d}t$, which yields: $F(t) = \rho\pi r^2(t)V^2$. The maximum impact force F_0 is reached for $r(t) = R$. Hence we get:

$$F_0 = \pi\rho R^2 V^2 \quad (1)$$

This expression can be seen as a dynamic pressure ρV^2 applied over a surface area πR^2. It can also be understood as arising from the deceleration (from V to 0) of a mass $M = 4\pi\rho R^3/3$ in a time $2R/V$. When compared to experiments, eqn (1) is observed (in dashed lines) to nicely fit the different data in Fig. 2 without any adjustable parameter.

In order to complement this first study, we now consider a simpler (and cheaper) sensor, namely a thin glass lamella (Menzel-Glaser Microscope cover slip #1) of Young modulus $E =$ 69 GPa, density $\rho_g = 2350$ kg m^{-3}, thickness $h = 160$ μm, and transverse width $b = 24$ mm. One side is clamped by squeezing 10 mm of a 60 mm-long lamella between two thick glass plates. The other side being free, we have a narrow rectangular plate of length $L = 50$ mm and mass $M = \rho_g hbL$, free to vibrate. Since the drop spreads at impact, the impact location is adjusted a few millimeters from the tip of the plate in order to avoid spilling. We observe plate oscillations after impact, and typical results (again captured with a high-speed camera) are reported in Fig. 3 (and ESI Movie 2†), where the vertical position of the free end of the lamella is shown as a function of time, for different impact speeds. The dynamics of the plate is dominated by its first mode of vibration, as shown by the time-evolution of the motion of the plate's tip (Fig. 3).

Focusing on the maximum force, we denote δ_0 as the largest deformation of the lamella for a given impact. We plot this quantity in Fig. 4a as a function of impact speed for water drops of different radii, and compare in Fig. 4b the plate deflection between water and Galinstan for $R = 1.3$ mm. The results contrast with Fig. 2 since we now observe that δ_0 varies linearly with both V and ρ.

At mechanical equilibrium, the deflection δ_0 of a thin plate is proportional to the applied force F_0 ($\delta_0 \sim F_0L^3/EI$ where $I = bh^3/12$ is the moment of inertia of the plate). With an impact force varying as V^2 (as seen before), we anticipate a deflection quadratic in velocity. It is not the case here because the plate has a slow response compared to the crashing time $2R/V$ ($\approx$1 ms) of the liquid: the characteristic time $\tau_0 = 1/f_0$ of the plate in Fig. 3b is about 20 ms, and it is expected to be a function of the plate parameters ($\tau_0 = (EI/ML^3)^{-1/2}$). The lamella is not at static equilibrium during an impact ten times shorter than its response time, and we cannot assume instantaneous proportionality between deformation and force. Before impact, the drop of mass m moves at speed V and the plate of mass M is at rest. After impact, the drop sticks to the plate, resulting in a system of mass (m + M) vibrating at its natural frequency, independent of the collision speed V. With a uniform distribution of m along the plate, the first resonance frequency would become $f = f_0\left(\frac{M}{M+m}\right)^{1/2}$. A geometrical correction could be introduced to take into account the fact that the drop is neither localized at the free end, nor homogeneously spread all over the lamella. However, since $m \ll M$, this correction is marginal, and we assume $f \approx f_0$. The lamella is vibrating on its natural mode, with a parabolic modal shape as a first approximation for clamped free end conditions. Hence its momentum can be written $p_M = \int_0^L \rho_g bh\ 2\pi f_0\delta_0\frac{x^2}{L^2}\cos(2\pi f_0 t)\mathrm{d}x = \frac{2\pi}{3}Mf_0\delta_0\cos(2\pi f_0 t)$. On the other hand, the momentum of the drop vibrating at the tip of the lamella is: $p_m = m2\pi f_0\delta_0\cos(2\pi f_0 t)$. Assuming that the

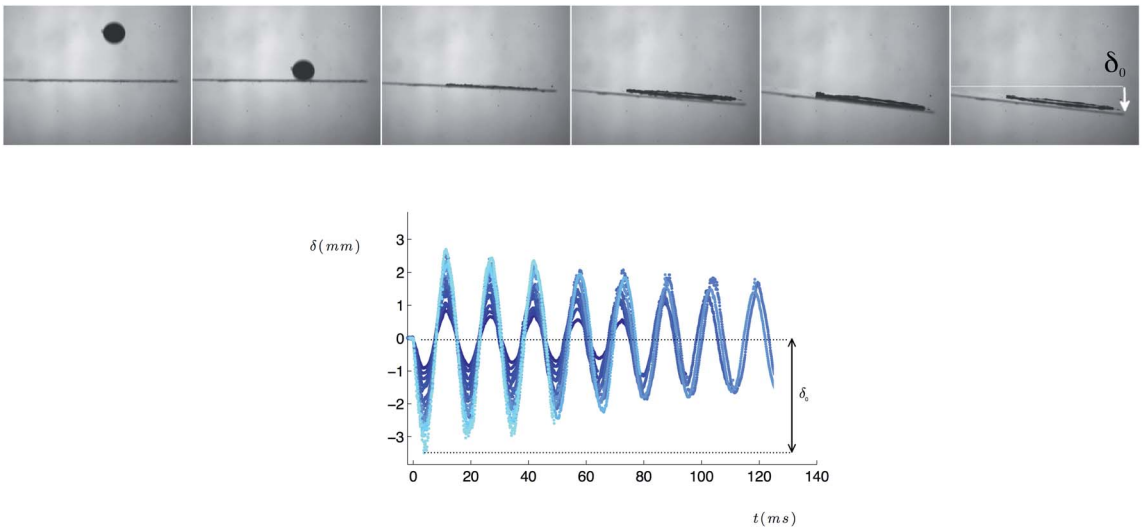

Fig. 3 (a) Galinstan drop of radius $R = 1.25$ mm and speed $V = 4$ m s^{-1} hitting the edge of a thin glass plate. Images are separated by 1 ms. We denote δ_0 as the maximum plate deflection after impact. Each image only shows 1/3 of the lamella. (b) Vertical deflection δ of the lamella tip as a function of time for experiments such as shown in (a). Each curve corresponds to an impact speed V (the brighter, the higher V, which varies from 1.3 m s^{-1} to 4.9 m s^{-1} by steps of 0.3 m s^{-1}). The characteristic time of vibration of the plate is independent of V and observed here to be $\tau \approx 20$ ms.

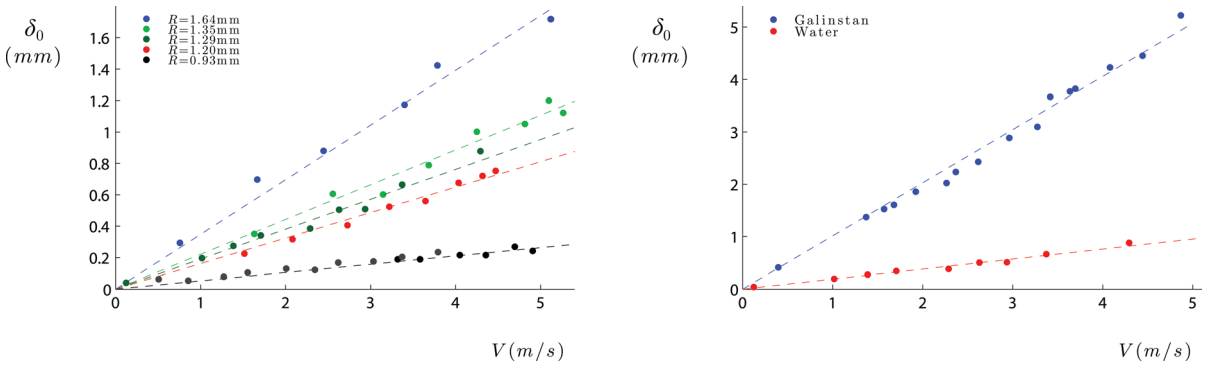

Fig. 4 (a) Maximal deflection δ_0 of the tip of a glass lamella as a function of the impacting speed of a water drop hitting this lamella close to the edge. We do not observe a parabolic relationship between δ_0 and V, but a linear law. (b) Comparison between water (lower curve) and Galinstan (upper curve) for a radius $R = 1.3$ mm. The ratio of δ_0 between the liquids is approximately the ratio of their densities.

first mode accounts for the dynamics also at $t = 0$, the conservation of momentum yields for $m \ll M$:

$$\delta_0 \approx \frac{3}{2\pi}\frac{m}{M}\frac{V}{f_0} \quad (2)$$

In order to explore a large range of densities, we repeated the experiment with the previous liquids (water, Galinstan) to which we added acetone (of density $\rho = 714$ kg m^{-3}), hexane ($\rho = 659$ kg m^{-3}) and a viscous silicone oil ($\rho = 970$ kg m^{-3}, viscosity of 500 mPa s). We show in Fig. 5 how the deflection δ_0 rescaled by the distance V/f_0, as suggested by the model, varies as a function of the ratio m/M of both masses, for all experiments. As predicted by eqn (2), data collapse on a line of slope 1.

According to the characteristic response time τ_0 of the substrate, we expect two regimes of impact: (i) a fast one, where the liquid crash is quicker than the response of the substrate, which leads to eqn (2); (ii) a slow one, where the impact is slower than τ_0. In the latter case, the response of the plate is quasi-static (mechanical equilibrium) and the deformation proportional to the force: δ_0 scales as L^3F_0/EI, which yields using eqn (1): $\delta_0 \sim \pi\rho R^2V^2L^3/EI$, quadratic in velocity. Since τ_0 is a function of L, let us re-express the transition between both regimes in terms of substrate length: the linear regime in V occurs for $L > L_c$, and the quadratic one for $L < L_c$ where the critical length L_c is given by:

$$L_c \sim \left[\frac{Eh^2}{\rho_g}\right]^{1/4}\left[\frac{R}{V}\right]^{1/2} \quad (3)$$

For glass lamellae and millimetric drops in our range of impact speeds, this critical length is around 3 cm. Since the lamellae in the experiments ($L = 5$ cm) are longer than L_c, we indeed expect $\delta_0(V)$ to be linear, as observed.

Leaves can be viewed as lamellae with a large response time τ_0, owing to an effective Young modulus E more than one thousand times smaller than for glass. For a leaf (of thickness h and width b comparable to that of our lamellae), L_c is about 6 mm. Most plants have leaves longer than L_c, so that eqn (2) can be used to estimate the deflection of leaves under rain. For millimetric drops on leaves of a few centimeters ($\tau_0 \approx 600$ ms, $f_0 \approx 1.5$ Hz), eqn (2) predicts centimetric deflections. But eqn (2) also exhibits the sensitivity to other parameters of the leaf: bigger drops hitting thin small leaves can generate a deflection comparable to the leaf size, which can lead to breakage after multiple impacts.

The two sensors studied here were shown to have different behaviors when exposed to impacting drops. We can think of exploiting these results to discuss how force measurements provide an estimate of drop radii, a quantity of interest in meteorology where it is desired to access the polydispersity of falling rain. We assume that the drops reach the sensor with their terminal velocity V_0,[25,26] for which inertial friction in air balances the liquid weight. These two forces can be written as $4\pi\rho R^3g/3$ and $\rho_aC_x\pi R^2V^2/2$ respectively where ρ_a is the density of the air, and $C_x \approx 0.44$ the drag coefficient (at Re > 1000.) Hence we get: $V \sim (\rho Rg/\rho_a)^{1/2}$. Using this expression in eqn (1) yields:

$$F_0 \sim \frac{\rho}{\rho_a}mg \quad (4)$$

This formula emphasizes how the impact force magnifies the drop weight of raindrops (by a factor ρ/ρ_a, on the order of

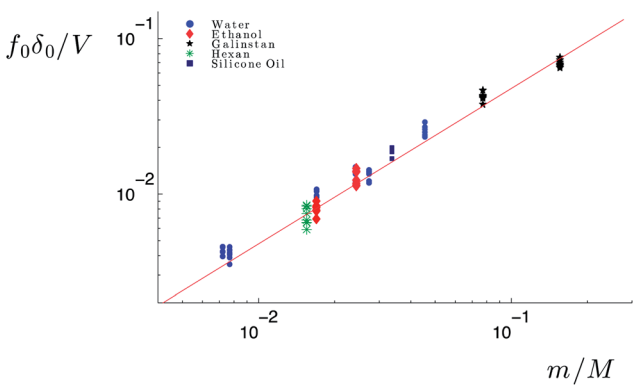

Fig. 5 Normalized deflection $f_0\delta_0/V$ as a function of the ratio m/M between the drop and the plate mass. V varies from 20 cm s^{-1} to 6 m s^{-1}. The red line shows equation $y = (3/2\pi)x$, that is, eqn (2). Each color corresponds to a liquid, and each cluster to different radii R between 0.9 and 1.7 mm.

1000), which shows why measuring the impact force can be a precise method to obtain the drop mass. Alternatively, we could also access the maximum deflection δ_0 for raindrops impacting lamellae. For instance, for lamellae of length $L > L_c$, we obtain after expressing the terminal velocity of raindrops in eqn (2):

$$\delta_0 \sim \frac{\rho^{3/2} g^{1/2}}{{\rho_a}^{1/2} M f_0} \cdot R^{7/2} \quad (5)$$

The deflection δ_0 can be measured from a side view video, from which we can deduce $R \sim {\delta_0}^{2/7}$. By associating several sensing plates (hydrophobically coated in order to avoid cleaning between successive impacts), we can assess the polydispersity of rain.

We can finally estimate the collision energy. The system periodically transfers bending energy $Ebh^3{\delta_d}^2/L^3$ into kinetic energy $E_{\text{k-plate}} = 1/5\,[1/2M(\delta_0 2\pi f_0)^2]$, that is, $(9m/5M)E_{\text{k-drop}}$. The kinetic energy $E_{\text{k-drop}}$ of a rain drop is around 1 mJ and the energy of the plate after impact is typically 10^{-4} J. Assuming an efficiency of 10% when transforming bending energy into electrical energy with a piezo-sensor, and supposing that this energy is delivered for each vibration, we get a transmitted power of 10^{-3} W. In the case of rain, assuming an impact every 10 seconds, we deduce that a roof of 100 m^2 with 10^6 receivers can deliver an average power of 100 W, just enough to light a bulb – a modest amount. Even if raindrops fall from high, drag slows them down dissipating almost all their potential energy, which is not efficient if we dreamt of energy harvesting but a blessing for plants, soil or living creatures that luckily experience relatively less impact force or erosion!

Acknowledgements

We thank Alexandre Ponomarenko for kindly sharing his Master thesis[27] and for enlightening discussions. We also thank Sunny Jung and Claude Basdevant for inspiring discussions.

References

1 S. S. Cook, Erosion by water-hammer, *Proc. R. Soc. London, Ser. A*, 1928, **119**, 481–488.
2 A. Yarin, Drop impact dynamics: splashing, spreading, receding, bouncing, *Annu. Rev. Fluid Mech.*, 2006, **38**, 159–192.
3 A. M. Worthington, The splash of a drop, *Society for Promoting Christian Knowledge*, London, 1895.
4 J. Eggers, M. A. Fontelos, C. Josserand and S. Zaleski, Drop dynamics after impact on a solid wall: theory and simulations, *Phys. Fluids*, 2010, **22**, 062101.
5 L. Xu, W. W. Zhang and S. R. Nagel, Drop splashing on a dry smooth surface, *Phys. Rev. Lett.*, 2005, **94**, 184505.
6 T. Tran, H. J. J. Staat, A. Prosperetti, C. Sun and D. Lohse, Drop Impact on Superheated Surfaces, *Phys. Rev. Lett.*, 2012, **108**, 036101.
7 R. Kannan and D. Sivakumar, Drop impact process on a hydrophobic grooved surface, *Colloids Surf., A*, 2008, **317**, 694–704.
8 P. Tsai, M. H. W. Hendrix, R. R. M. Dijkstra, L. Shui and D. Lohse, Microscopic structure influencing macroscopic splash at high Weber number, *Soft Matter*, 2011, **7**, 11325–11333.
9 T. Deng, K. K. Varanasi, M. Hsu, N. Bhate, C. Keimel, J. Stein and M. Blohm, Nonwetting of impinging droplets on textured surfaces, *Appl. Phys. Lett.*, 2009, **94**, 133109.
10 X. Li, X. Ma and Z. Lan, Dynamic Behavior of the Water Droplet Impact on a Textured Hydrophobic/Superhydrophobic Surface: The Effect of the Remaining Liquid Film Arising on the Pillars' Tops on the Contact Time, *Langmuir*, 2010, **26**, 4831–4838.
11 M. Nearing, J. Bradford and R. Holtz, Measurement of force *vs.* time relations for waterdrop impact, *Soil Sci. Soc. Am. J.*, 1986, **50**, 1532–1536.
12 M. Nearing and J. Bradford, Relationships between waterdrop properties and forces of impact, *Soil Sci. Soc. Am. J.*, 1987, **51**, 425–430.
13 A. C. Imeson, R. Vis and E. de Water, The measurement of water-drop impact forces with a piezo-electric transducer, *Catena*, 1981, **8**, 83–96.
14 A. K. Dickerson, P. G. Shankles, N. M. Madhavan and D. L. Hu, Mosquitoes survive raindrop collisions by virtue of their low mass, *Proc. Natl. Acad. Sci. U. S. A.*, 2012, **109**, 9822–9827.
15 O. G. Engel, Waterdrop collisions with solid surfaces, *J. Res. Natl. Inst. Stand. Technol.*, 1955, **5**, 281–298.
16 H. M. Kwon, A. Paxson, K. Varanasi and N. Patankar, Rapid Deceleration-Driven Wetting Transition during Pendant Drop Deposition on Superhydrophobic Surfaces, *Phys. Rev. Lett.*, 2011, **106**, 036102.
17 J. E. Field, J.-J. Camus, M. Tinguely, D. Obreschkow and M. Farhat, Cavitation in impacted drops and jets and the effect on erosion damage thresholds, *Wear*, 2012, **290**, 154–160.
18 S. Thoroddsen, T. Etoh, K. Takehara, N. Ootsuka and Y. Hatsuki, The air bubble entrapped under a drop impacting on a solid surface, *J. Fluid Mech.*, 2005, **545**, 203–212.
19 S. Thoroddsen, K. Takehara and T. Etoh, Micro-splashing by drop impacts, *J. Fluid Mech.*, 2012, **706**, 560–570.
20 M. Mani, S. Mandre and M. P. Brenner, Events before droplet splashing on a solid surface, *J. Fluid Mech.*, 2010, **647**, 163–185.
21 A. S. Grinspan and R. Gnanamoorthy, Impact force of low velocity liquid droplets measured using piezoelectric PVDF film, *Colloids Surf., A*, 2010, **356**, 162–168.
22 R. K. Dadashev, R. Kutuev, D. Elimkhanov and Z. Bichueva, Surface tension ofindium–tin–gallium melts, *Russ. J. Phys. Chem. A*, 2007, **81**, 1734–1737.
23 Q. Xu, E. Brown and H. M. Jaeger, Impact dynamics of oxidized liquid metal drops, *Phys. Rev. E: Stat., Nonlinear, Soft Matter Phys.*, 2013, **87**, 043012.

24 S. Mangili, C. Antonini, M. Marengo and A. Amirfazli, Understanding the drop impact phenomenon on soft PDMS substrates, *Soft Matter*, 2012, **8**, 10045–10054.
25 R. Gunn and G. Kinzer, The terminal velocity of water drops and raindrops in stagnant air, *J. Meteorol.*, 1949, **6**, 243–248.
26 E. Reyssat, Gouttes, films et jets: quand les écoulements modèlent les interfaces, PhD Thesis, Université Paris Diderot, Paris, 2007.
27 A. Ponomarenko, Impacts sur des surfaces flexibles, Master Thesis, Université Pierre et Marie Curie, Paris, 2008.